

# NATIONAL ADVISORY COMMITTEE FOR AERONAUTICS

TECHNICAL NOTE 3316

SOME MEASUREMENTS OF NOISE FROM THREE  
SOLID-FUEL ROCKET ENGINES

By Leslie W. Lassiter and Robert H. Heitkotter

Langley Aeronautical Laboratory  
Langley Field, Va.



Washington

December 1954

AFMDC  
TECHNICAL LIBRARY  
AFL 2811



## NATIONAL ADVISORY COMMITTEE FOR AERONAUTICS

## TECHNICAL NOTE 3316

SOME MEASUREMENTS OF NOISE FROM THREE  
SOLID-FUEL ROCKET ENGINES

By Leslie W. Lassiter and Robert H. Heitkotter

## SUMMARY

A systematic investigation of the sound field of a 1,000-pound-thrust solid-fuel rocket was made and data on two other rockets, of 900 and 5,500 pounds of thrust, were obtained at a few isolated field points. Frequency spectra for the range 20 to 15,000 cps indicate that the noise of each rocket is random, with a spectrum envelope which peaks in the lower part of the audible range. Angular distributions of overall sound pressure in the frequency range 0 to 40 cps and 20 to 20,000 cps indicate a similarity to subsonic jet-noise distribution, with the maximum pressures occurring at angles of  $30^\circ$  to  $45^\circ$ , respectively, off the jet axis downstream of the nozzle.

## INTRODUCTION

The noise from various types of jets has for the past several years attracted a great deal of attention. The bulk of the research effort in this field has been directed toward the noise from subsonic and choked converging nozzles, since installations utilizing such nozzles, namely, the turbojet engines, are encountered most frequently. References 1 to 4 are typical of the work which has been done along these lines. However, except for the discussion in reference 5 and the brief mention in references 6 and 7, the noise from rocket engines, utilizing supersonic nozzles, has not been reported.

It is becoming apparent that due consideration must be given to the noise from rockets since their applications are increasing in number. At present, rocket noise is particularly a problem in assisted-take-off operations of airplanes and in missile-launching operations. There are also the potential problems of structural buffeting and malfunctioning of avionic equipment in proximity to the rocket exhaust. The purpose of the present report, therefore, is to provide some information as to the intensity, spectrum, and directivity characteristics of rocket noise.

The data were obtained partly from routine thrust-stand firings and partly from a series of firings concerned only with noise evaluation. From the data obtained from the latter firings, a systematic investigation of the sound field was made; in the routine thrust-stand firings, only isolated measurements of spectrum and intensity were possible. The data are believed to be of interest both in regard to fundamental jet-noise research and in regard to evaluation of specific problems of rocket operation. An appendix is included which outlines the procedure for adjusting to unit band width the noise spectra obtained with a Panoramic Sonic Analyzer.

### SYMBOLS

B	band width, cps
D	nozzle diameter, in.
F	thrust, lb
f	frequency, cps
$\bar{I}$	overall-sound-pressure level, db
$I_B$	pressure level of a frequency band B, db
$I_f$	spectrum level of sound pressure (per cycle band width), db/cycle
$\bar{p}$	overall sound pressure, $\left(\sum p_f^2 df\right)^{1/2}$ , dynes/cm <sup>2</sup>
$p_B$	pressure of a frequency band B, db
$p_f$	sound pressure (per cycle band width), dynes/cm <sup>2</sup>
z	distance from nozzle, ft
$\psi$	azimuth angle, deg
Subscripts:	
e	exit conditions
t	throat conditions

## APPARATUS AND METHODS

Configurations tested.- Sound measurements were made during test-stand firing of a number of rockets of three kinds. Some of the physical characteristics of these rockets (hereinafter referred to as rockets A, B, and C) are given in the following table:

TABLE I

Rocket-engine designation	Number of rockets fired	Thrust, lb	Chamber pressure, lb/sq in. abs	Exit pressure, lb/sq in. abs	Exit diameter, in.	Exit Mach number	Exit velocity, fps
A	6	1,000	1,950	39.0	1.625	3.16	5,340
B	1	900	1,090	11.3	2.375	3.48	5,700
C	1	5,500	1,092	19.6	6.180	3.57	6,540

Rocket chamber pressure, as given in the table, is the average value existing between ignition and burnout. A time history of chamber pressure during a firing will ordinarily indicate a gradually changing mean value, upon which are superimposed fluctuations, of the order of  $\pm 25$  lb/sq in., which are presumably due to burning irregularities in the propellant.

Exit pressure is given because of its significance in determining the flow conditions at the nozzle exit. The exit pressure, which depends upon both the diffuser geometry and the chamber pressure, may be above or below atmospheric - that is, the flow may be underexpanded or overexpanded. With the different conditions of expansion are associated widely different flow patterns which might be expected to influence the noise generation, but the extent of the effects is not known.

Propellant geometry is another factor which may be significant. In all the rockets tested, an external inhibitor was employed; that is, burning of the propellant from its outer lateral surface inward was prohibited. In rocket A, burning progressed along the axis of the propellant away from the nozzle. The propellant of rocket B had a tapered tubular perforation, or opening, of circular cross section extending through the center; thus, burning occurred over the full length of the propellant and progressed radially outward from the perforation. The propellant of rocket C had a full-length star-shaped perforation.

Test conditions.- The tests were made under two different sets of conditions at the field points shown in figure 1(a). The firings of rocket A were made with the rockets strapped to a concrete test bed as shown in the left-hand part of figure 1(b). The test bed placed the

rocket center line parallel to the ground and about 1.5 feet above ground level in a field which had no sizeable sound-reflecting objects within approximately 100 yards of the rocket. The firings of rockets B and C were made with the rockets strapped to test beds inside a test cell closed on three sides with heavy concrete walls and overhead with a light-weight metal roof. The right-hand part of figure 1(b) gives a schematic plan view of this test site and indicates the positions of the rockets for testing. Rocket B was oriented with its center line parallel to the ground and about 1 foot above it; rocket C was also oriented parallel to the ground at a height of about 3.5 feet.

Measurements made.- Figure 1(a) illustrates the coordinate system used and the field points at which data were obtained for each rocket. Overall sound-pressure readings and tape recordings were obtained at two points in the sound field from each firing. The recordings were later analyzed to provide spectrum analyses.

Instrumentation.- A schematic diagram of the instrumentation used is shown in figure 2. In order to obtain data over the frequency range 0 to 20,000 cps, each of the sound-pressure measurement systems was composed of two parts: one part responding to components from 20 to 20,000 cps and the other to components from 0 to 40 cps. These are illustrated in the left-hand part of figure 2. For the range 20 to 20,000 cps, a crystal-type sound measurement system was used for detection. Its output was observed on a vacuum-tube voltmeter from which overall levels were obtained. At the same time the overall signal was attenuated, monitored, and recorded by a tape recorder for later frequency analysis. The frequency response of the tape recorder limited the upper frequency cutoff to 15,000 cps and the lower frequency cutoff to about 50 cps.

Frequency analyses in the range 50 to 15,000 cps were obtained by playback of the recordings into a Panoramic Sonic Analyzer, the screen of which was photographed continuously during some 30 trace sweeps to obtain a time average. This procedure provided permanent records from which spectrum levels could be obtained by the method discussed in the appendix. Overall levels from the tape recorder were checked against the direct readings obtained from the vacuum-tube voltmeter at the time of firing.

For the range 0 to 40 cps, an NACA miniature electrical pressure gage (ref. 8) and low-pass filter unit was used as the microphone. After demodulation of the signal from its carrier, it was channeled to a rectifier-type voltmeter for overall level determination and to a pen recorder.

Frequency analysis of one of the pen records (0 to 40 cps) was made with the help of a crude system designed to translate the frequencies up to a range where the Panoramic Sonic Analyzer could be used. In order

to do this, a segment of the record was inked black on one side of the deflection curve, placed on a circular drum, and rotated at a speed one-hundred times that at which the recording was made. The moving paper was scanned by a fine line of light, which reflected from the paper to a photocell pickup. Variations in total illumination reaching the photocell produced an electrical signal that was analyzed by the Panoramic Sonic Analyzer. Frequency calibrations and drum-speed factors were then applied to obtain quantitative results.

## PRESENTATION OF RESULTS

### Noise From Rocket A

Six rockets of type A were fired and successive firings were monitored by a portable sound-level meter at a fixed position in order that possible variations in noise among the rockets might be taken into account. The overall sound levels obtained from this monitor system indicated very consistent operation among the various rockets; the maximum difference was 2.5 decibels, and for five out of the six rockets fired the scatter was within 0.5 decibel.

As indicated in table I presented previously in the section entitled "Configurations tested," these rockets operate at an exit pressure which is higher than atmospheric and hence are underexpanded.

Angular distribution of overall pressure.- The spatial distributions of pressure magnitude in the frequency ranges 0 to 40 cps and 20 to 20,000 cps are given by the polar plots of figure 3, obtained at a distance of 50 feet, which corresponds to approximately 370 exit diameters, from the nozzle. The curve of figure 3(a), for the frequency range 0 to 40 cps, indicates that the noise is strongly directional, with the angle of maximum pressure at about  $30^\circ$  off the flow axis. The distribution curve for the frequency range 20 to 20,000 cps, in figure 3(b), likewise indicates strong directivity, but with the angle of maximum pressure at a larger value ( $45^\circ$ ).

Noise spectra.- Sample spectrum envelopes of the noise from rocket A are given in figure 4. These envelopes were obtained from the Panoramic Sonic Analyzer records and have been adjusted to a unit band width by the procedure discussed in the appendix. The spectra are of random character, similar to those observed in reference 6, and indicate a peak frequency that varies from about 150 to 300 cps as the azimuth angle changes from  $15^\circ$  to  $165^\circ$ . With the exception of the spectrum at  $45^\circ$ , this shifting of the peak frequency is continuous and in qualitative agreement with results from subsonic jet-noise tests.

## Noise From Rockets B and C

Rocket B. - Data on rocket B were obtained from a single firing and therefore are limited to only two stations:  $90^\circ$  and 3 feet (15 diameters) and  $26^\circ$  and 15 feet (75 diameters). These distances are observed to be appreciably smaller than those used for rocket A and, hence, the two sets of data may not be directly comparable. It should be noted also that the presence of the test-cell walls, as shown in figure 1, may have some effect on these measurements. This effect is probably small, however, because of the highly directional radiation pattern of rocket noise. (See fig. 3.)

Figure 5 illustrates the spectra obtained with rocket B. Like those of rocket A, these spectra have been adjusted to a unit-band-width basis for presentation. A single data point from the low-frequency system is used for the frequency range below 40 cps. In figure 5, pressure levels at  $90^\circ$  have been adjusted by the inverse-square-law relationship to correspond to a distance of 15 feet for comparison with the data at  $\psi = 26^\circ$ . At both azimuth angles, the spectra are somewhat broader and flatter than those of figure 4 for rocket A; nevertheless, they have a fairly well defined peak. At  $26^\circ$  the peak is at about 850 cps and at  $90^\circ$  the peak is at about 1,500 cps. These frequencies are observed to be more than five times as high as those of rocket A at comparable angles even though rocket B has the larger exit diameter.

Rocket C. - Data from rocket C were also obtained from a single firing and, because of the presence of deflected control vanes in the flow at the nozzle exit, are not necessarily representative. However, these data are included here to give at least an indication of the order of magnitude for this type of rocket.

Figure 6 gives the form of the spectra and the overall levels obtained at angles of  $30^\circ$  and  $60^\circ$ , at a distance of 15 feet. At  $60^\circ$  the spectrum is somewhat similar to those of the other two rockets; that is, it has a clearly defined peak which, in this case, occurs at about 1,000 cps. The low-frequency analysis, by the method previously discussed, indicates that below 40 cps the spectrum level lies at much lower values and does not change much between 1 and 30 cps. The spectrum for the  $30^\circ$  azimuth, on the other hand, indicates that here the components below 100 cps are greatest, since the spectrum envelope continues to rise with decreasing frequency. Unfortunately, the low-frequency noise-measuring system did not yield reliable data at this azimuth angle.



## DISCUSSION OF RESULTS

Although the measurements reported herein are not complete enough to allow any detailed conclusions to be drawn, comparison of the data with the fairly well established characteristics of subsonic jet noise (refs. 1 to 4) seems in order. In general, the frequency spectra of all the rockets tested are similar to those of subsonic jets in that they are random and have an envelope with a single peak in the lower part of the audible range. This peak varies with azimuth angle in much the same manner as for subsonic jets; that is, it tends to occur at higher frequencies as azimuth angle is increased.

The directivity characteristics of rocket noise, as indicated for rocket A by figure 3, seem to be consistent with subsonic jet-noise characteristics. In both, the maximum radiation is at an acute angle off the jet axis downstream of the nozzle. The angle is somewhat larger for rocket noise,  $45^\circ$  as compared with about  $30^\circ$  for a turbojet, but this difference is probably to be expected because of the much higher velocity and speed of sound in the rocket exhaust. Reference 4 indicated that the angle was dependent upon those two parameters. The tendency for the low-frequency lobe to have its maximum at a smaller angle than the high-frequency lobe is also consistent with subsonic jet-noise data, which indicated that the lower the frequency band considered the more closely the lobe oriented itself to the jet axis.

The pressure level of noise at a given azimuth angle from a subsonic jet increases with approximately the 4th power of jet velocity and is essentially independent of nozzle diameter if measurements are made at a given number of diameters away. The nature of the present rocket-noise investigation was not such as to afford any evidence as to whether or not this relation holds for rocket noise. However, as shown in figure 16 of reference 7, rocket-noise pressure levels, despite their high intensity, are some 15 decibels lower than extrapolation by the 4th-power law of subsonic jet-noise data to rocket velocities would indicate. The acoustic efficiency is correspondingly lower too. From integration of the angular distribution pattern of overall pressure, rocket A was found to be 1/4 percent efficient; whereas, a subsonic turbojet has been shown (ref. 6) to be about 1 percent efficient under full-load conditions. These differences may be evidence of the significance of turbulence level involved in jet mixing since, as discussed in references 9 and 10, the inherently greater stability and smaller spreading angle of a supersonic jet imply that this jet is less turbulent than a subsonic jet.



As discussed in the section entitled "Apparatus and Methods," the effects of propellant configuration, the underexpansion or overexpansion of the flow, and the chamber-pressure fluctuations are difficult to assess. These appear to be factors which will require detailed study under controlled conditions for evaluation of their effects.

#### CONCLUDING REMARKS

Although specific conclusions regarding rocket noise are difficult to draw from the rather limited measurements reported herein, certain characteristics are apparent. Each of the three rockets tested produced spectra somewhat similar to those of subsonic jets, that is, random and with an envelope which peaks in the lower part of the audible range. The directional characteristics appear to be about the same as were observed with subsonic jets also, since the maximum pressure occurs at angles of  $30^\circ$  to  $45^\circ$  off the jet axis downstream of the nozzle.

Langley Aeronautical Laboratory,  
National Advisory Committee for Aeronautics,  
Langley Field, Va., September 2, 1954.

## APPENDIX

PROCEDURE FOR ADJUSTING TO UNIT BAND WIDTH THE NOISE SPECTRA  
OBTAINED WITH A PANORAMIC SONIC ANALYZER

The Panoramic Sonic Analyzer used for spectrum analysis in the present investigation requires a correction to its indicated spectrum if the spectrum level in decibels per cycle is desired. The need for a correction arises from the fact that the band width of the instrument is not constant but increases with frequency. An instrument of this type tends to accentuate the higher frequency components because the root-mean-square value  $p_B$  of a band of frequency components is proportional to the square root of band width  $B$  as follows:

$$p_B = \sqrt{B p_f^2} \quad (1)$$

where  $p_f$  is the unit-cycle value. For example, figure 7 illustrates the Panoramic Sonic Analyzer response to an impressed white-noise signal in which the mean amplitude is essentially constant from 20 cps to 20,000 cps. The distortion of the spectrum as presented by the instrument is evident.

A correction curve for converting the indicated spectrum to the true spectrum in decibels per cycle can be obtained from figure 7, however, if a measurement of the band width at some given frequency is available. Figure 8 shows the measured band width at 100 cps. From this curve a nominal band width (between half-power frequencies) is found to be 53.5 cps. Thus, from equation (1), the spectrum level  $p_f$  at 100 cps is

$$p_f = \frac{p_B}{\sqrt{53.5}} = (0.136) p_B$$

This factor of 0.136 between the unit-band-width value  $p_f$  and the indicated value  $p_B$  corresponds to a -17.2-decibel correction to be applied to  $p_B$ .

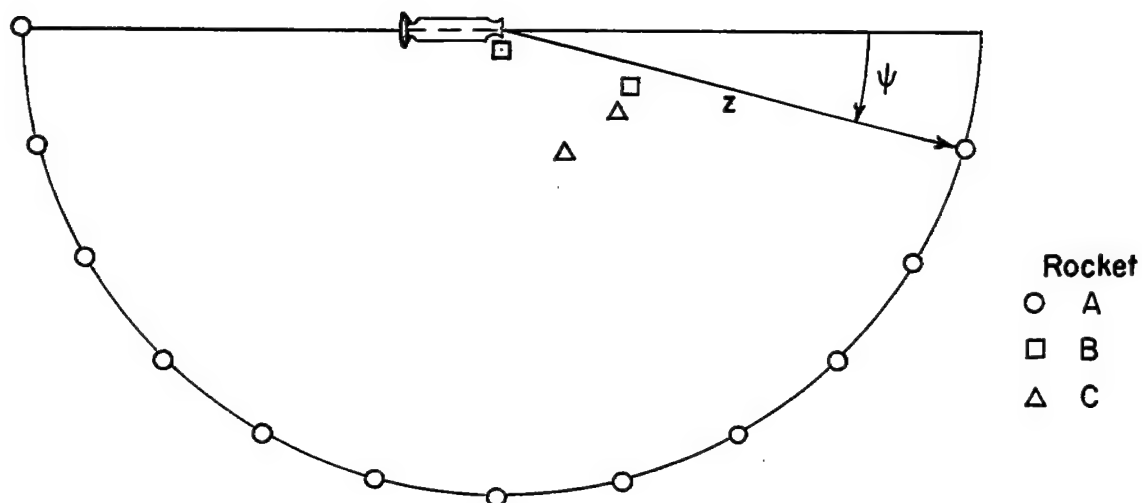
Although this same procedure could be carried out at various frequencies throughout the range to obtain a correction curve, it is not necessary because figure 7 already gives all the information necessary to determine the correction at any given frequency relative to that at 100 cps. Thus, adding to 17.2 decibels the difference in mean deflections (as measured in fig. 7) between 100 cps and any given frequency

gives the overall correction curve for the instrument. Figure 9 gives this curve, which was used to obtain all the spectrum levels given in the present paper.

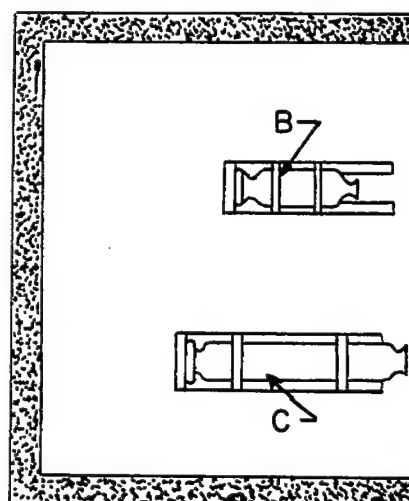
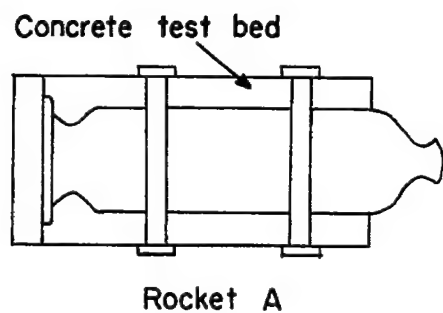
As a check against this method, one of the rocket-noise records was analyzed by another means and the results were compared with the results obtained with the Panoramic Sonic Analyzer. Figure 10 gives that comparison. The solid-line curve at the top of the figure is the spectrum envelope as indicated by the Panoramic Sonic Analyzer (uncorrected). The corrected Panoramic envelope is given by the long-dashed curve at the bottom of the figure. A slight shifting of the spectrum peak is seen to occur in the correction process. The short-dashed curve is the spectrum level as obtained from a 30-cps constant-band-width analyzer (corrected to unit band width); this method of analyzing the records should yield an envelope which most nearly approximates the true spectrum and the corrected Panoramic envelope is seen to be in general agreement with it. Some of the sharpness of the peak is lost in the analysis of the Panoramic Sonic Analyzer and the spectrum level is generally a few decibels lower, but for the purposes of the present paper the corrected analysis is considered to be sufficiently accurate.

## REFERENCES

1. Powell, Alan: A Survey of Experiments on Jet Noise. Aircraft Engineering, vol. XXVI, no. 299, Jan. 1954, pp. 2-9.
2. Westley, R., and Lilley, G. M.: An Investigation of the Noise Field From a Small Jet and Methods for Its Reduction. Rep. No. 53, College of Aero., Cranfield (British), Jan. 1952.
3. Greatrex, F. B.: Engine Noise. Jour. R.A.S., vol. 58, no. 520, Apr. 1954, pp. 223-231.
4. Lassiter, Leslie W., and Hubbard, Harvey H.: Experimental Studies of Noise From Subsonic Jets in Still Air. NACA TN 2757, 1952.
5. Bolt, R. H., Lukasik, S. J., Nolle, A. W., and Frost, A. D., eds.: Handbook of Acoustic Noise Control - Volume I. Physical Acoustics. WADC Tech. Rep. 52-204 (Contract No. AF 33(038)-20572), Wright Air Dev. Center, U. S. Air Force, Dec. 1952.
6. Von Gierke, H. E.: Physical Characteristics of Aircraft Noise Sources. Jour. Acous. Soc. Am., vol. 25, no. 3, May 1953, pp. 367-378.
7. Regier, Arthur A.: Why Do Airplanes Make Noise? SAE Preprint No. 284, SAE Nat. Aeronautic Meeting (New York), Apr. 12-15, 1954.
8. Patterson, John L.: A Miniature Electrical Pressure Gage Utilizing a Stretched Flat Diaphragm. NACA TN 2659, 1952.
9. Gooderum, Paul B., Wood, George P., and Brevoort, Maurice J.: Investigation With an Interferometer of the Turbulent Mixing of a Free Supersonic Jet. NACA Rep. 963, 1950. (Supersedes NACA TN 1857.)
10. Lighthill, M. J.: On Sound Generated Aerodynamically - II. Turbulence as a Source of Sound. Proc. Roy. Soc. (London), ser. A, vol. 222, no. 1148, Feb. 23, 1954, pp. 1-32.



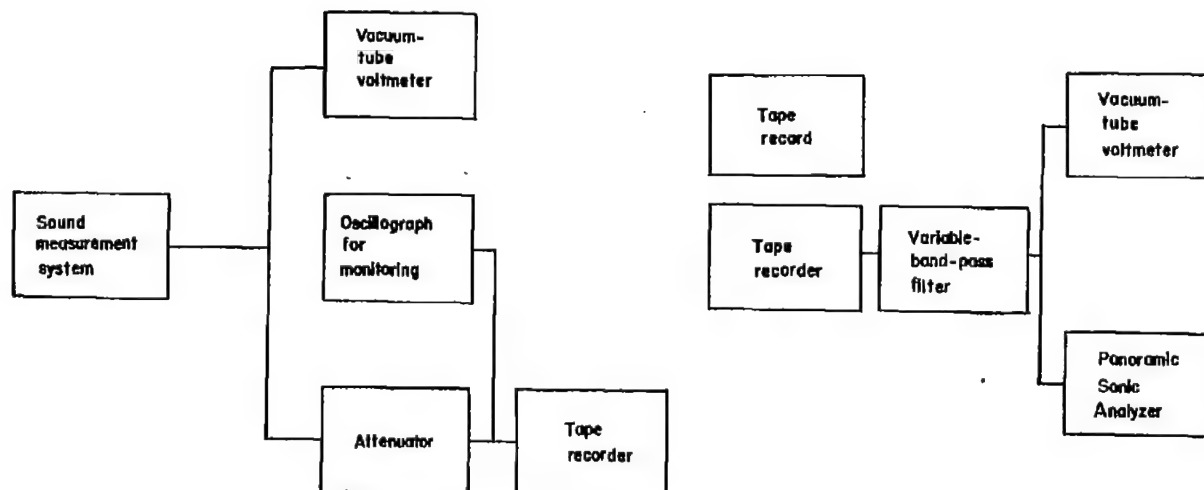
(a) Coordinate system.



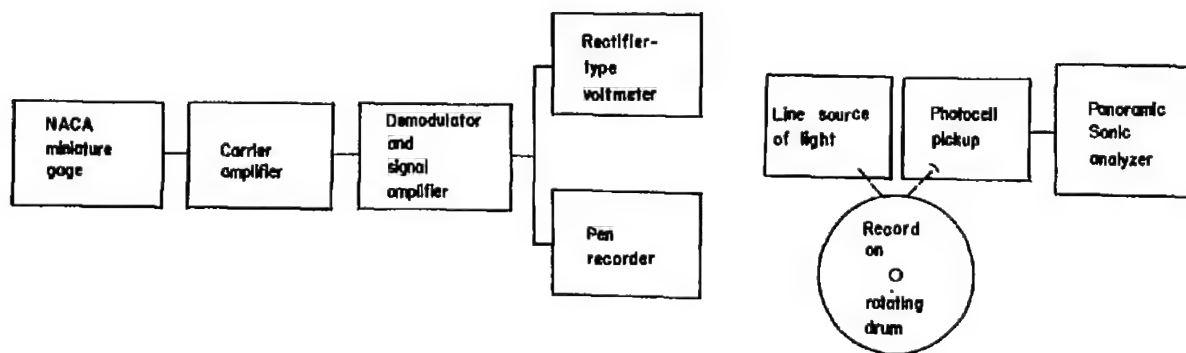
Rockets B and C

(b) Test stands.

Figure 1.- Coordinate system and schematic diagram of test stands for rocket-noise tests.

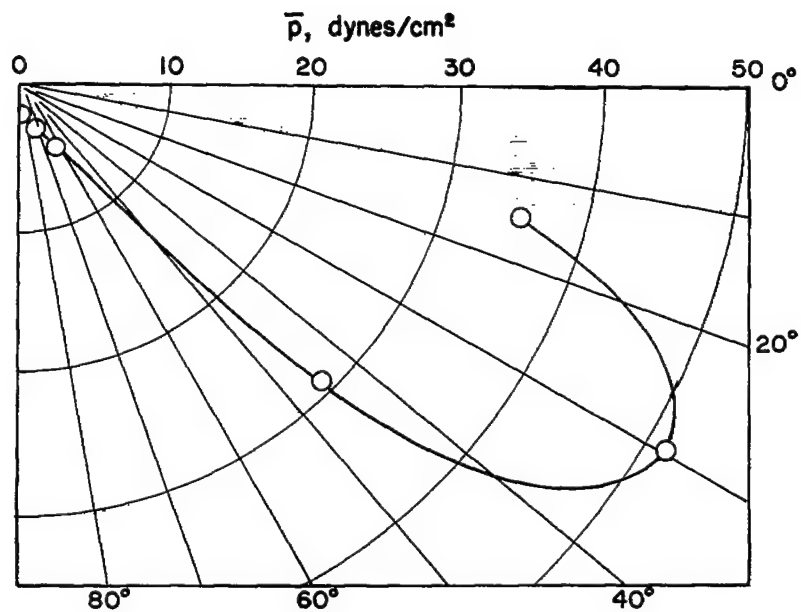


(a) 20 to 20,000 cps.

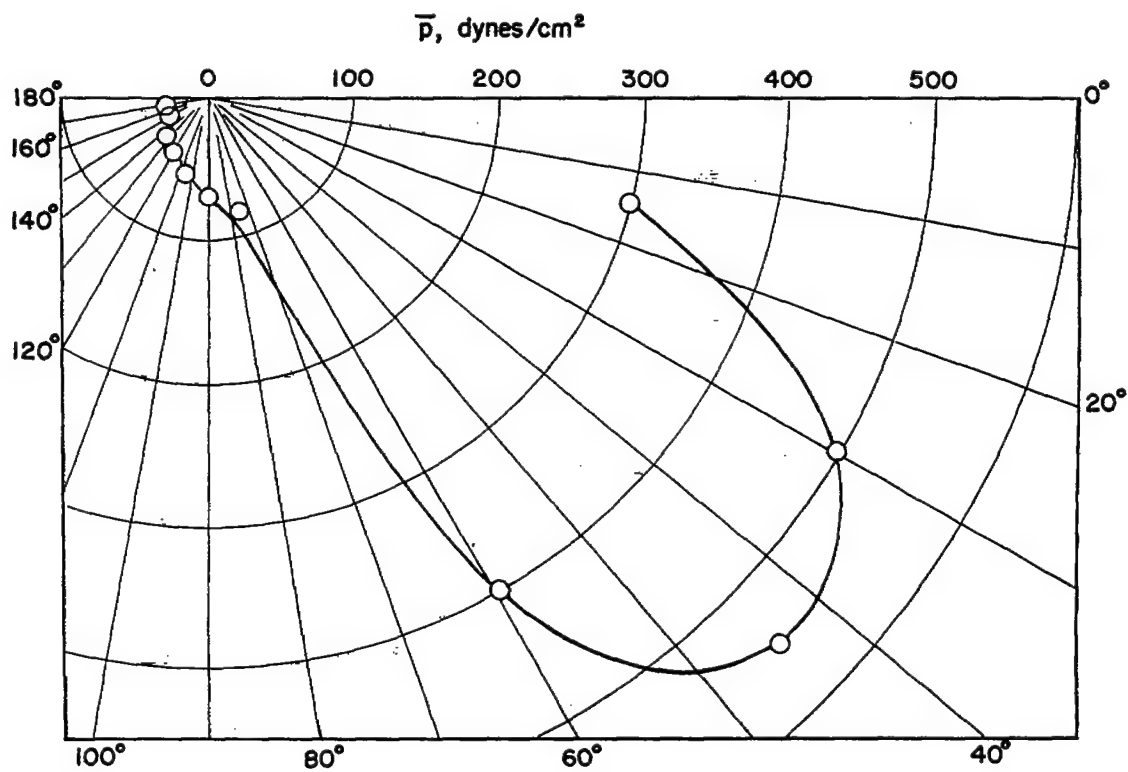


(b) 0 to 40 cps.

Figure 2.- Instrumentation for rocket-noise investigation.



(a) 0 to 40 cps.



(b) 20 to 20,000 cps.

Figure 3.- Angular distribution of sound pressure from rocket A.  
 $z = 50$  feet;  $F = 1,000$  pounds.



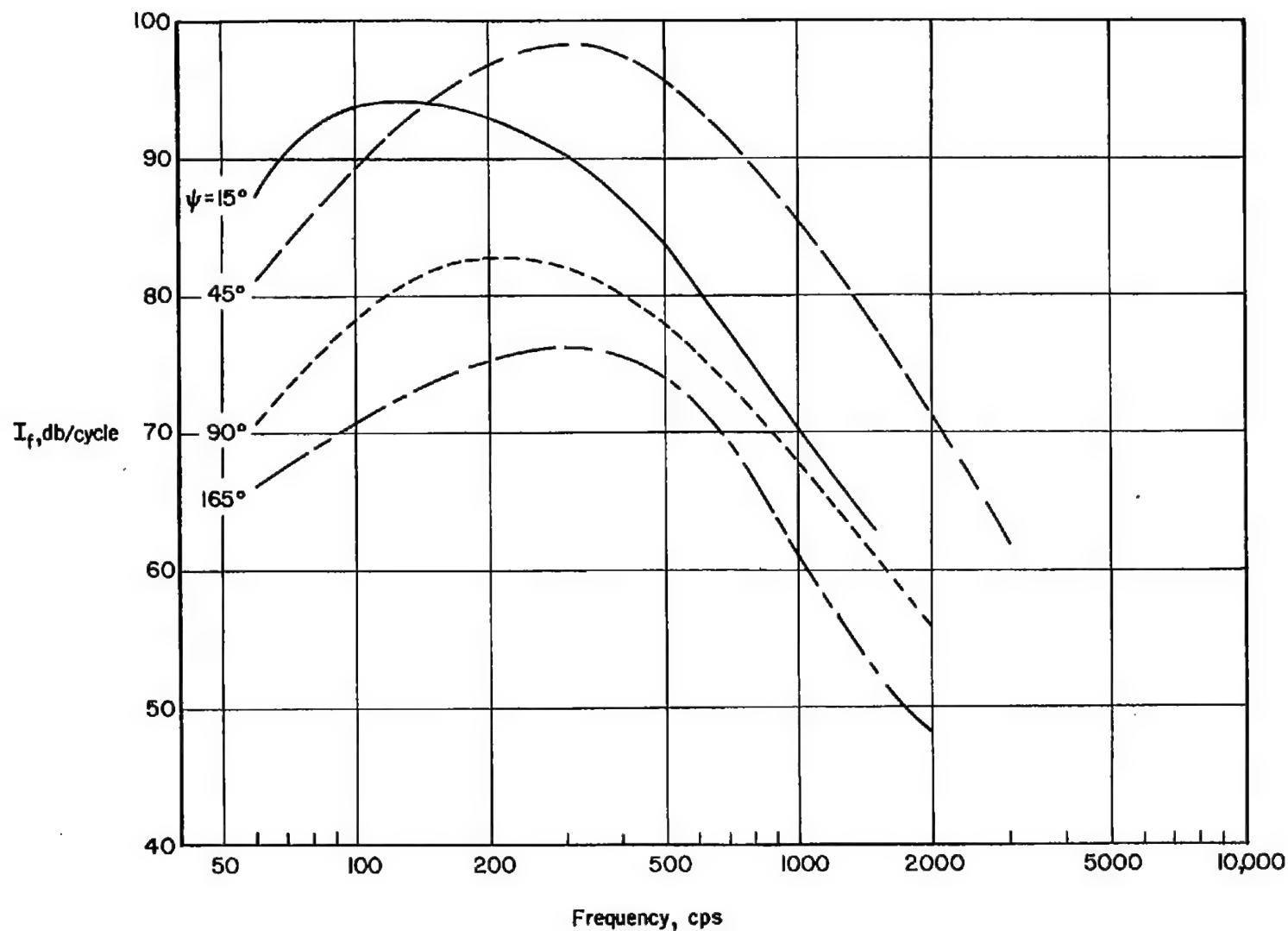


Figure 4.- Frequency spectra of noise from rocket A.  $z = 50$  feet;  
 $D_t = 0.64$  inch;  $D_e = 1.625$  inches;  $F = 1,000$  pounds.

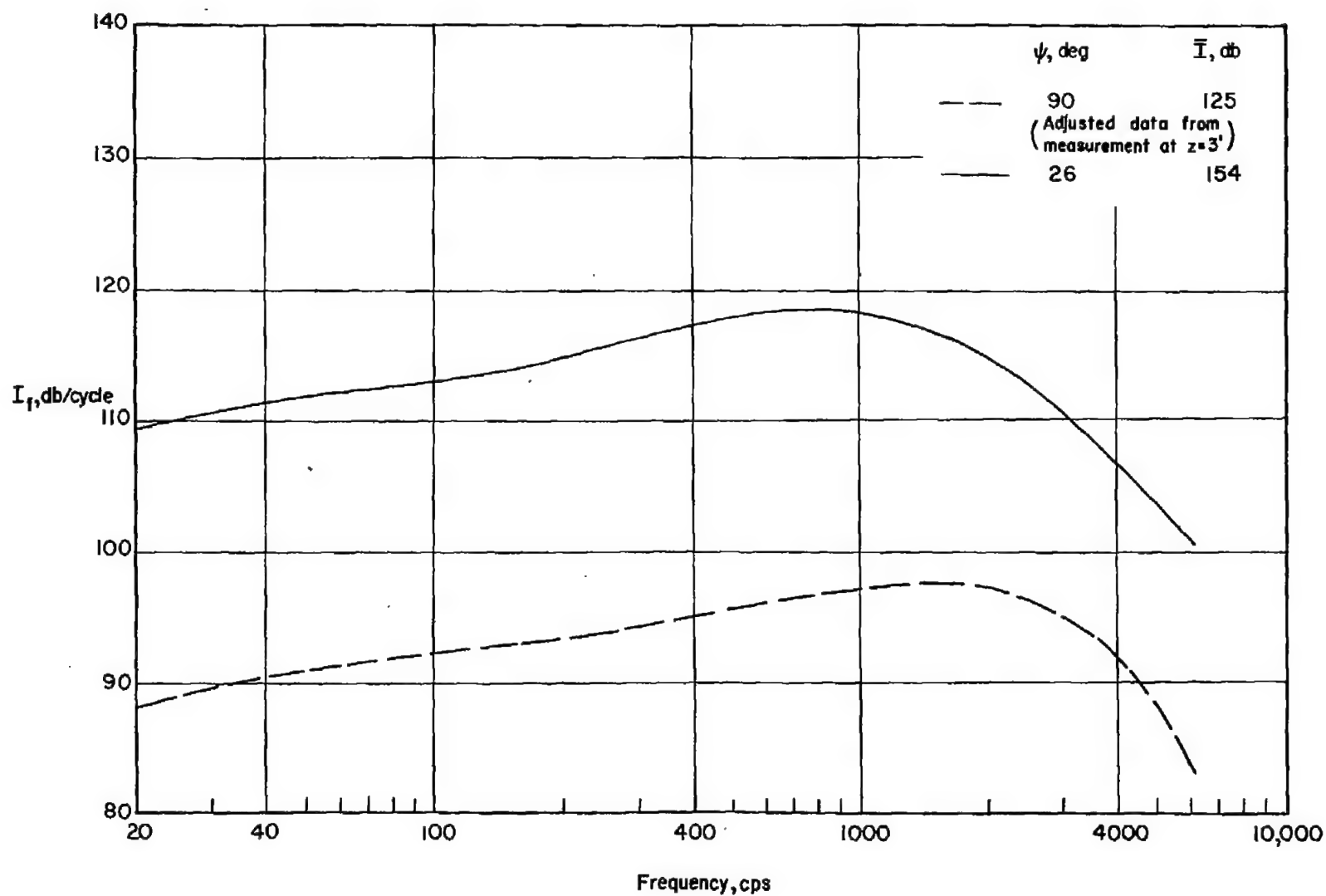


Figure 5.- Frequency spectra of noise from rocket B.  $z = 15$  feet;  
 $D_t = 0.75$  inch;  $D_e = 2.375$  inches;  $F = 900$  pounds.

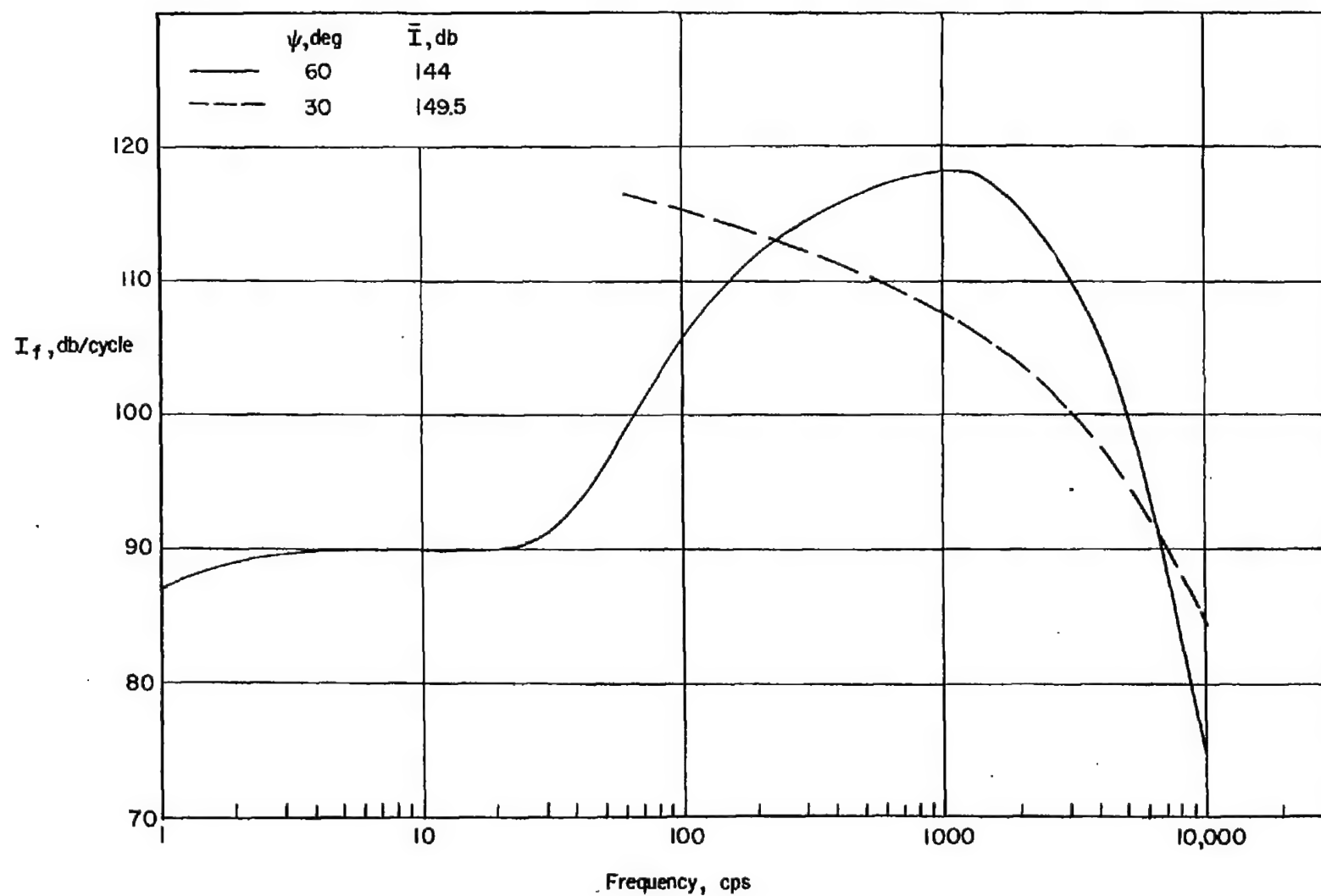


Figure 6.- Frequency spectra of noise from rocket C.  $z = 15$  feet;  
 $D_t = 2.43$  inches;  $D_e = 6.18$  inches;  $F = 5,500$  pounds.

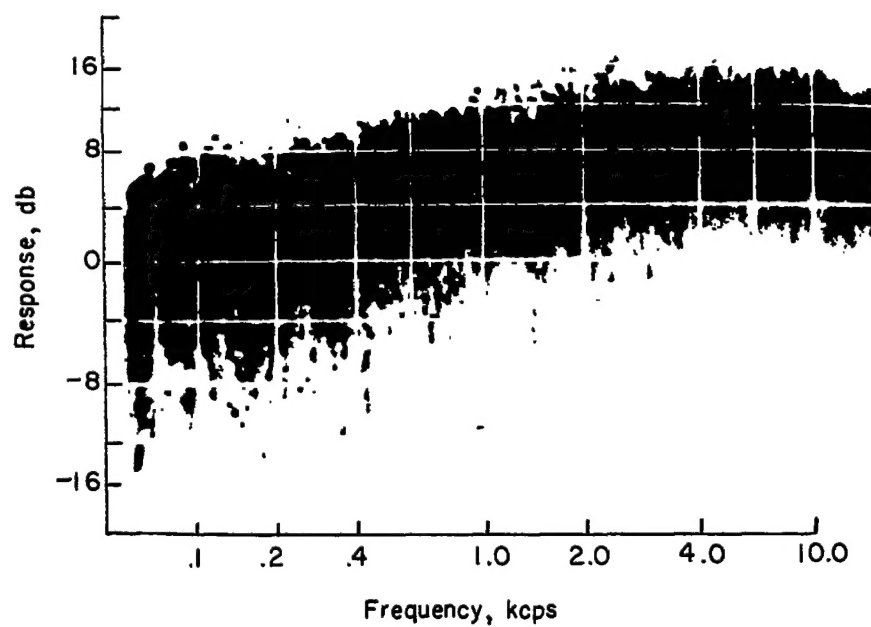


Figure 7.- Panoramic analysis of white-noise signal.

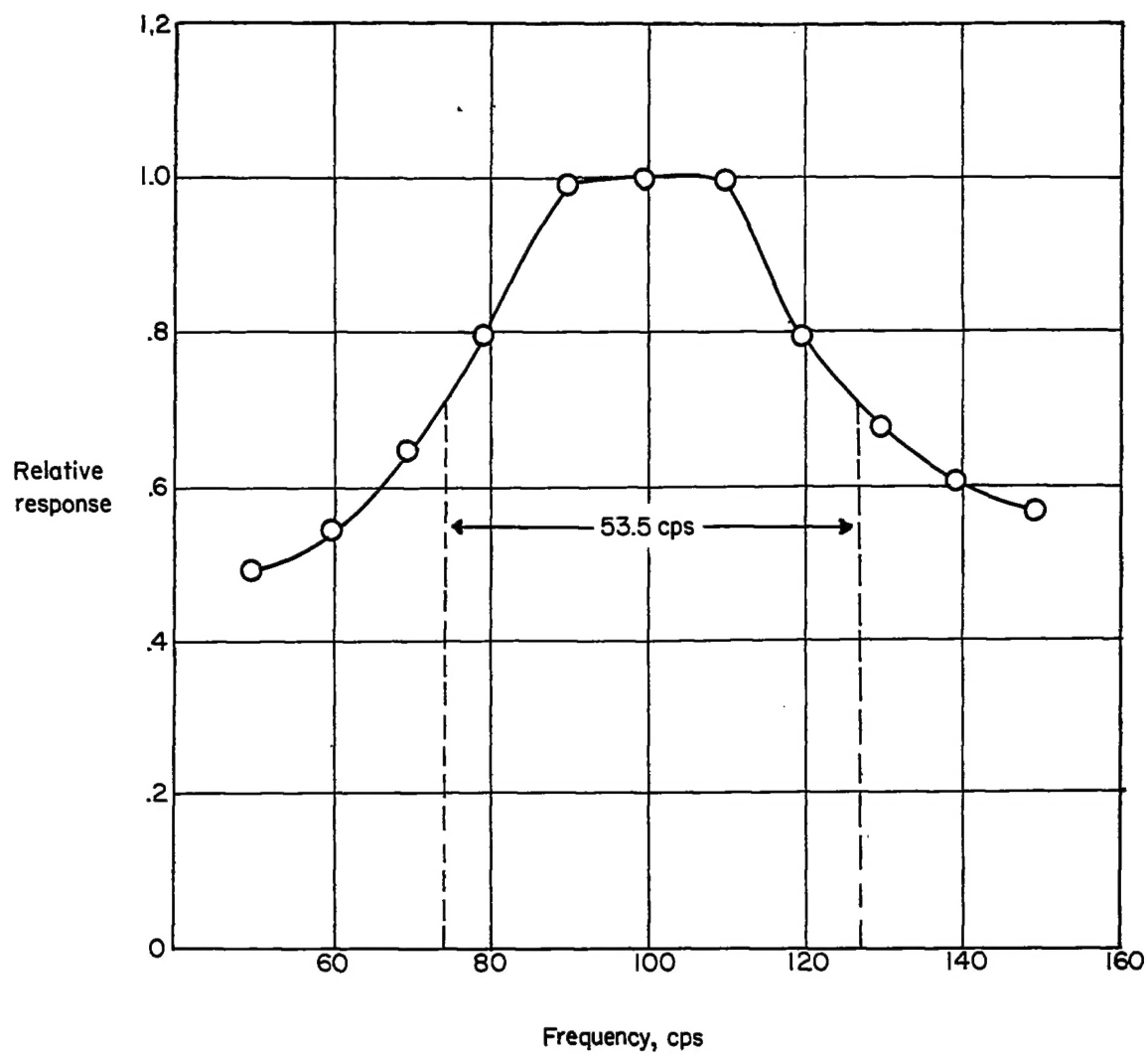


Figure 8.- Band width of Panoramic Sonic Analyzer at 100 cps.

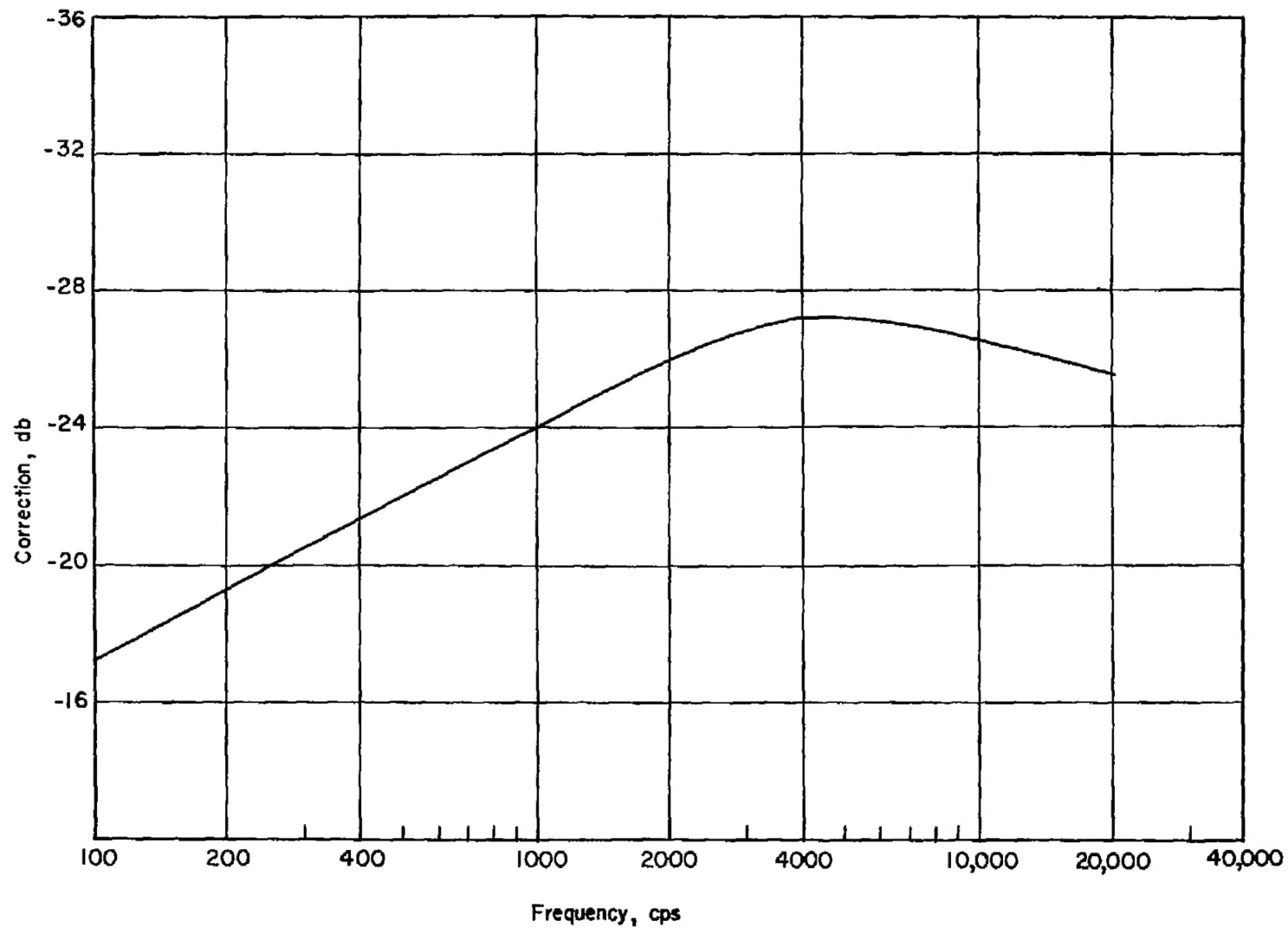


Figure 9.- Correction curve for converting the indications from the Panoramic Sonic Analyzer to decibels per cycle.

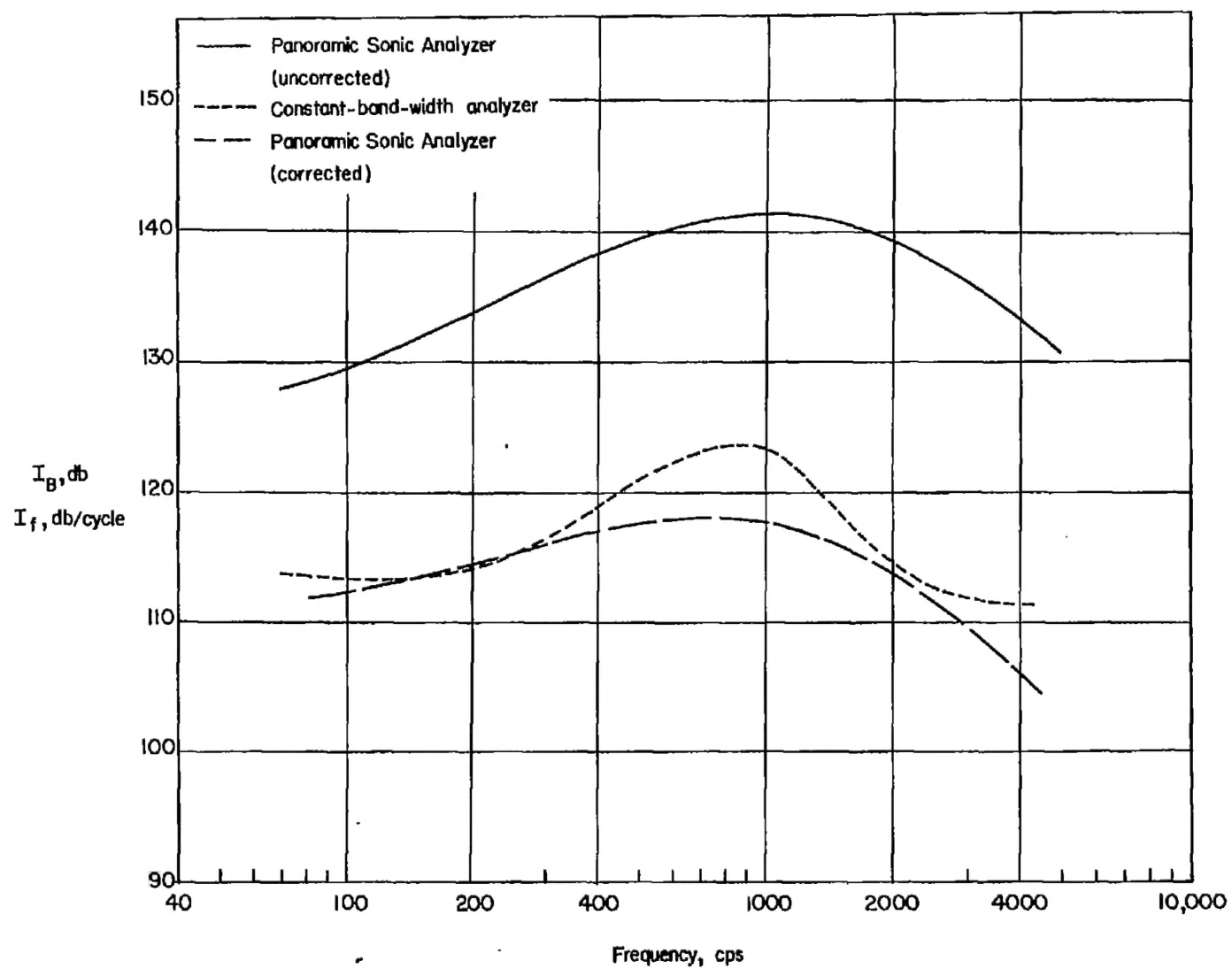


Figure 10.- Analysis of noise from rocket B with various analyzers.